Spatial and Temporal Heterogeneity of Regional Pulmonary Blood Flow in Piglets

THOMAS V. BROGAN, JAMES D. MELLEMA, LYNN D. MARTIN, MELISSA KRUEGER, GREGORY J. REDDING,
AND ROBB W. GLENNY

*Department of Pediatrics [T.V.B., J.D.M., L.D.M., G.J.R.] and Department of Anesthesiology [L.D.M.], Children's Hospital
and Regional Medical Center, Seattle, WA 98105; Department of Medicine [M.K.], and Departments of Medicine
and of Physiology and Biophysics [R.W.G.], University of Washington, Seattle, WA, 98105*

ABSTRACT: Regional pulmonary blood flow (PBF) in adult animals varies over space and time, following a fractal pattern. We hypothesized that PBF would follow a fractal pattern in young animals. Five, two-week old piglets were sedated and mechanically ventilated. After stabilization, fluorescent microspheres were injected *via* the right atrium at baseline and then again at 5, 20, 20.5, 40 and 60 min. The lungs were subsequently excised, dried, inflated, and cored into 0.12-cm^3 pieces (mean $n = 561 \pm 106$ per animal) with the spatial coordinates recorded for each piece. Regional PBF was spatially and temporally heterogeneous with a spatial coefficient of variation of $43.3 \pm 7.9\%$ and a temporal coefficient of variation of $14.3 \pm 0.4\%$. PBF followed a fractal pattern with a fractal dimension of 1.20 ± 0.06 at 20 min, remaining stable throughout the experiment. PBF decreased with distance from the hilum but did not follow a lobar pattern. Temporal heterogeneity did not significantly increase with time but low flow regions demonstrated the greatest temporal variability throughout the study. Hence, PBF in young piglets was characterized both spatial and temporal heterogeneity. (*Pediatr Res* **62:** 434–439, 2007)

A considerable amount of information describing the structural and functional characteristics of the pulmonary circulation during postnatal lung development exists. Features such as vascular reactivity, pulmonary capillary recruitment, and metabolic capabilities of the microvasculature appear to differ between adult and immature animals (1–8). Recently, the fractal spatial distribution and isogravitational heterogeneity of pulmonary blood flow (PBF) have been delineated in adult animals using injectable microspheres that achieved greater resolution than earlier studies (9,10). The results of these studies diverge from the findings of homogeneous gravitational zones described by West *et al.* (11). Temporal heterogeneity also occurs in the pulmonary circulation, which may subserve the conservation of energetics rather than ventilation-perfusion relationships (12).

Hitherto, these physiologic characteristics remain unstudied in newborn or very young animals. Speculation suggests that the fractal nature of PBF is based on the pulmonary anatomy, particularly of the precapillary bed (13). If true, the spatial distribution of PBF in young animals should be similar to that in adults. Furthermore, the presence of temporal heterogeneity of PBF in young animals has not been reported. Previous studies suggest a higher degree of pulmonary vascular reactivity in neonatal animals (2,3,6) compared with adults, and hence temporal heterogeneity should be greater than that previously described in adult animals.

We measured spatial and temporal heterogeneity in piglets because morphometric studies of pulmonary development in the piglet suggest that the vascular and alveolar changes during the first 3 months of life are similar to those seen in humans (14,15). We hypothesized that under normoxic conditions the pulmonary blood flow would demonstrate greater spatial heterogeneity due to smaller piece sizes than used in studies of adult animals. In addition, we expect a greater degree of temporal heterogeneity due to the greater pulmonary vasoreactivity.

METHODS

The University of Washington Animal Care Committee approved the study protocol. Piglets, studied in the supine posture, were anesthetized with intramuscular ketamine (30 mg/kg) and xylasine (4 mg/kg), then with i.v. sodium pentobarbital (20 mg/kg). Anesthesia was maintained with intermittent boluses of sodium pentobarbital (10 mg/kg). Anesthesia was initially assessed by conjunctival reflex response and by following vital signs after neuromuscular blockade. Animals received neuromuscular blockade with intermittent boluses of pancuronium bromide (0.3 mg/kg). A tracheostomy was performed. Ventilation was administered with a Harvard small animal ventilator (Harvard Apparatus, Boston, MA). The animals were ventilated with air and tidal volumes (Vt) of 10–12 mL/breath at a rate of 22–28 breaths per minute to maintain arterial Pco$_2$ (PaCO$_2$) of approximately 35–40 torr. Once appropriately set, ventilation was not changed throughout the remainder of the experiment. A thermodilution pulmonary artery catheter *via* the internal jugular vein and a carotid artery catheter were placed. Hemodynamic parameters and arterial blood gases were monitored throughout the experiment. Temperature was monitored with a pulmonary artery thermister.

Regional pulmonary blood flow was measured using injectable fluorescent microspheres (1×10^6) of 15 μM-diameter (FluosSpheres; Molecular Probes, Eugene, OR, USA) of seven different colors (orange, blue-green, crimson, blue, yellow-green, red, scarlet). The microspheres were vortexed and sonicated before use and injected *via* the right atrium over a 30-s period followed by a 10-mL saline flush. One color was injected at each time point in the study. The color order was randomized across animals.

Protocol. After stabilization on the ventilator, the animals had baseline measurements (time 0) recorded including temperature, hemodynamic parameters (HR, mean systolic BP, mean pulmonary artery pressure (PAP), pulmonary artery occlusion pressure, cardiac output (Q)), and arterial blood gases. Simultaneously, one color of fluorescent microspheres was injected in the

Abbreviations: CV$_{spatial}$, spatial correlation of variation; **CV$_{temporal}$,** temporal correlation of variation; **PBF,** pulmonary blood flow

right atrium through the proximal port of the pulmonary artery catheter. Measurements and different color microsphere injections were then repeated at 5, 20, 40, and 60 min. Another injection was performed 30 s after the 20-min injection to evaluate temporal heterogeneity at different time intervals with no repeat in arterial blood gases. To assess the error secondary to the method, two colors of microspheres were injected simultaneously at the end of the experiment.

Following completion of the experiments, the animals were given i.v. heparin (1000 units), given an overdose injection of pentobarbital sodium (40 mg/kg) and exsanguinated. A sternotomy was performed, large-bore catheters were placed in the pulmonary artery and the left atrium and the thoracic aorta was tied off. The lungs were perfused with normal saline and 2% dextran (74,000 Da) until clear of blood, removed from the chest and allowed to dry inflated at an airway pressure of 25 cm H_2O.

When dry, the lungs were coated with Kwik foam (DAP Inc., Dayton, OH, USA), suspended vertically in a plastic-lined square box and embedded in rapidly setting urethane foam (908 g polyol and isocyanate; International Sales, Seattle, WA, USA) to create a rigid form to which a three-dimensional co-ordinate system could be applied. The foam block was cut into uniform slices. Each slice was placed on a grid with X (left to right) and y (ventral to dorsal) coordinates. The cored samples were 0.65 cm thick and 0.47 cm in diameter giving a volume of 0.12 cm^3. Each lung piece was assigned a three-dimensional co-ordinate and lobe designation and weighed. The fluorescent signal for each lung piece was determined by extracting the fluorescent dyes from each piece with an organic solvent and then measuring the concentrations of fluorescence in each sample using a luminescence spectrophotometer (Perkin-Elmer) then corrected for spillover (16).

The relative blood flow to each lung piece was divided by the weight of each piece and normalized to the mean, providing a relative weight-normalized fluorescence per piece. The relative blood flow was determined for each time point (microsphere injection). The data set for each piglet consisted of x, y, and z co-ordinates, lobe designation, weight and relative flow for each lung piece at each time point. Residual flow values from the mean for each lung piece were determined by subtracting the mean flow value per piece over time from the measured flow at each time point. Methodologic error was evaluated by simultaneous injections of two different colors.

Statistical analysis. Changes with time are analyzed *via* analysis of variance (ANOVA) with repeated measures. The Pearson correlation coefficient (*r*) calculated between perfusion at two time points is used to quantify the relationship between regional perfusion at different time points. The standard error of the estimate (SEE), which indicates the variation of residuals or "noise" about the fit of a linear model, is used to characterize the *r versus* time differences. Outliers in repeated observations over time are identified by fitting a multiple regression model to the observations and then exploring the residual from the model. The model included terms for pig-time (dummy variable), time and pig-time interaction. Standardized residuals >3.0 were considered outliers.

Relative blood flow to each piece is determined by the weight normalized measured fluorescence to that piece divided by the mean weight normalized fluorescence across all pieces within an animal. Coefficient of variation (CV = standard deviation/mean) characterizes the perfusion heterogeneity within each piglet. The coefficient of spatial variation (CV$_{spatial}$) is the SD of flow/average flow for all pieces at any one experimental time point. The CV is used rather than the SD (SD) so that variability relative to the mean is characterized. The CV is the variation from the mean pulmonary blood flow for all pieces of lung tissue sampled under a given condition.

The temporal variation for each piece (CV$_{temporal,i}$) is

$$CV_{temporal,i} = \sqrt{CV^2_{piece,i} - CV^2_{method,i}} \quad \text{(Eq. 1)}$$

Where CV$_{piece,i}$ is the total CV over time for each piece *i*. The relative methodological error in each piece i (CV$^2_{method,i}$) is estimated from the multiple time points by the formula

$$CV^2_{method,i} = 1/\sqrt{n} \quad \text{(Eq. 2)}$$

Where *n* is the mean number of microspheres in pieces across all injections. The average CV$_{temporal}$ is

$$CV_{temporal} = \sum CV_{temporal,i}/n \quad \text{(Eq. 3)}$$

Additionally a fractal analysis of the microsphere data for all piglets was performed for all conditions, following the method of Glenny and Robertson (16). Briefly, fractal analysis characterizes organ blood flow heterogeneity independent of scale of tissue sampled. Fractal dimension (*D*) is calculated from the coefficient of blood flow (CV) to individual pieces of lung. Small neighboring lung pieces are combined into a larger conglomerate piece based on multiplies (2, 3, 4, 6, 8, 12 16, 24, 32, 48, and 64) of the initial central piece size. The CV is then calculated as if the lung had been divided into the larger conglomerate pieces. Conglomerates are restricted to lie entirely within the right or left lung but may traverse lobes. The algorithm for dividing the lung is repeated for each conglomerate of size *n* pieces a total of *n* times, obtaining *n* coefficients of variation. The mean of the logarithm of the *n* CV is used for regression modeling to obtain *D*. The SD of the logarithm of the *n* CV is used for plotting error bars. The total number of conglomerate pieces for all $\sqrt{n}$ repetitions as the regression weight at piece size *n*. Log(CV) is plotted against log(piece size) and a regression line obtained using weighted regression analysis. *D* is calculated as (1 - slope) where slope was obtained from the regression line fitted to the log(CV) *versus* log(piece-size) data.

A total of $51 \pm 0.6\%$ of the lung by weight was sampled. A *p* value of <0.05 was considered statistically significant.

RESULTS

Five piglets weighing 3.5 ± 0.4 kg were studied. Blood gas data (Fig. 1) and hemodynamic conditions were stable throughout the course of the study in each animal with no point differing significantly from the values obtained at baseline (ANOVA for repeated measures, $p > 0.05$ for PaCO$_2$, Pao$_2$, HR, MAP, MPAP, PAOP and Q).

Data for PBF to the right upper lobe (rul) and middle lobe (rml) were combined due to poor demarcation between these lobes and inability to separate them during the coring process. The percentage of samples obtained from the left lower lobe, left upper lobe, right lower lobe, rul and cardiac lobe were 30.5%, 15.9%, 31.1%, 17.5% and 4.9%, respectively. The CV$_{spatial}$ was $43.4 \pm 7.9\%$ (Table 1) with individual CV$_{spatial}$ varying from 32.8 to 54.6%. The CV$_{spatial}$ for each animal varied by 5–19% (mean 8.8%) for measurements obtained 20 min apart. The fractal dimension for the piglets ranged from 1.19 ± 0.05 at 40 min to 1.22 ± 0.06 at baseline. A fractal dimension of between 1 and 1.5 defines the flow as fractal.
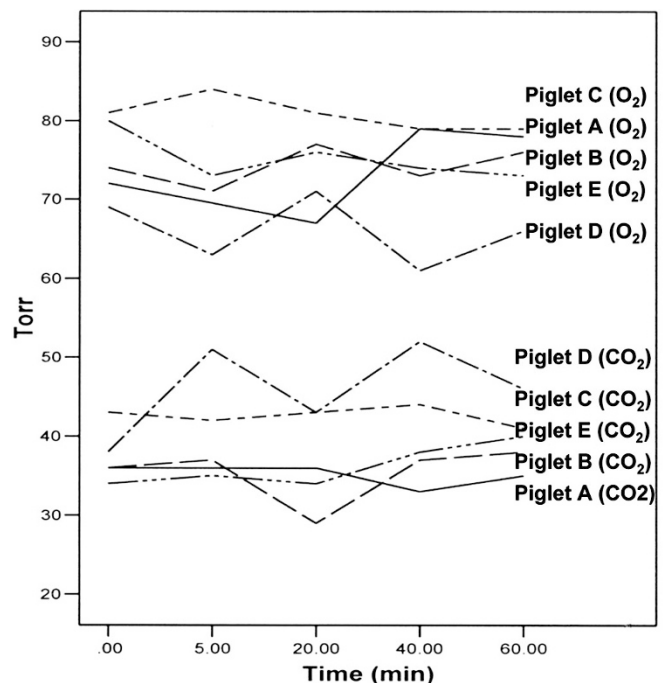

Figure 1. Gas-exchange measurements over time. Arterial Po$_2$ and Pco$_2$ for each animal just before injection of microspheres. Gas exchange remained constant in all animals throughout the study.

Table 1. *Microsphere data for piglets*

Animal	Lung Pieces	$CV_{temporal}$	$CV_{spatial}$
A	707	14.8	42.9
B	466	14.1	41.1
C	615	14.4	54.6
D	564	13.9	45.5
E	453	14.5	32.8
Mean (SD)	561 (106)	14.3 (0.4)	43.4 (7.9)

$CV_{temporal}$: Temporal coefficient of variation.
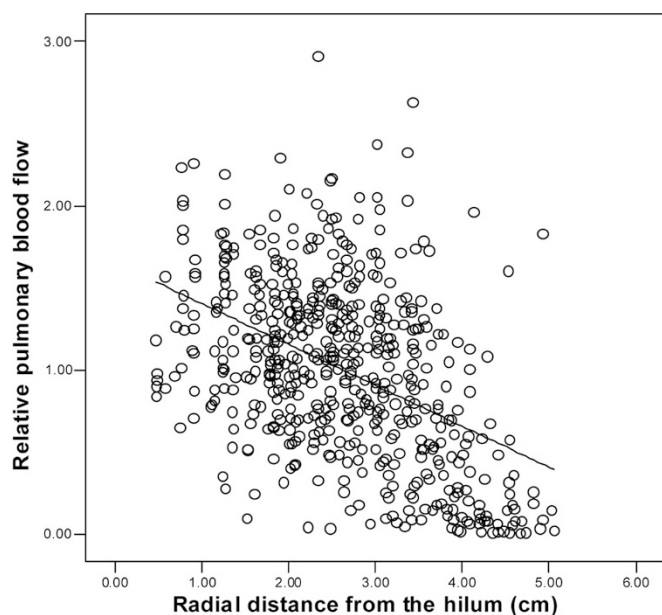$CV_{spatial}$: Spatial coefficient of variation.

Figure 2. Relative PBF decreases with distance from the hilum. Scattergraph of regional PBF *vs* radial distance from the hilum in centimeters (piglet C). The regression line shows the significant decline in pulmonary blood flow in with radial distance from the hilum. $y = -0.25 \times +1.66$; $R^2 = 0.21$.

Figure 3. The $CV_{spatial}$ increased with distance from the hilum. When divided arbitrarily into three regions, (0–1.85 cm from the hilum, 1.86–3.7 cm from the hilum and 3.71–5.55 cm from the hilum), the $CV_{spatial}$ of PBF increased significantly as radial distance from the hilum increased. Data from all animals have been combined (*$p < 0.05$ compared with first third of lung; **$p < 0.01$ compared with the proximal two thirds).

There was no statistical difference at any time point by ANOVA for repeated measures.

There was a decrease in the relative PBF with distance from the hilum under all experimental conditions (Fig. 2). All animals demonstrated a negative slope significantly with significant R^2 values of 0.12 ± 0.09 ($p < 0.001$). We also arbitrarily divided the lung into three sections moving radially away from the hilum to assess flow by regions. PBF decreased as radial distance from the hilum increased. Relative PBF was 1.11 ± 0.08 for pieces of lung 0 – 1.85 cm from the hilum. PBF decreased significantly to 1.05 ± 0.04 for pieces 1.86–3.7 cm from the hilum and 0.70 ± 0.19 for those pieces for 3.71–5.55 cm from the hilum. The decline in PBF away from the hilum was significant between all three groups ($p < 0.01$). In addition, the $CV_{spatial}$ increased significantly as distance from the hilum increased radially (Figure 3): $34 \pm 3\%$ for 0–1.85 cm from the hilum, $42 \pm 6\%$ for 1.86–3.7 cm from the hilum and $57 \pm 10\%$ for 3.71–5.55 cm from the hilum ($p < 0.001$ for the most distal third compared with the two proximal thirds, $p = 0.012$ for the second third compared with the first). Figure 4 shows that there was a significant tendency ($p < 0.01$) for flow to decrease up the lung (dorsal to ventral)
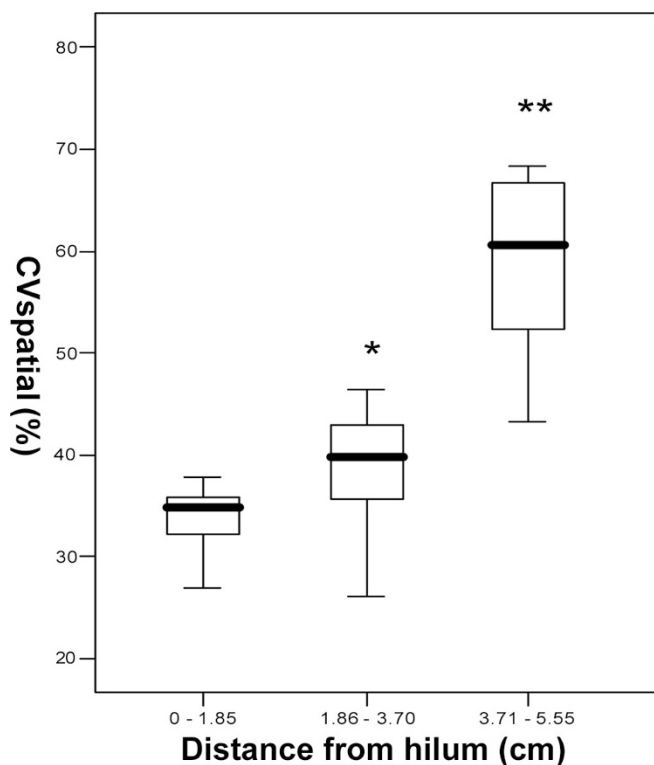
as well as along the lung (cephalad to caudad). Again, these anatomic patterns of pulmonary blood flow were stable throughout all experimental conditions.

The $CV_{temporal}$ ranged from 13.9 to 14.8% (table 1). There were no obvious patterns throughout the course of the experiment. Methodologic error in these experiments was evaluated by simultaneous injections of two different colors, which demonstrated differences in CV_{method} of $3.28 \pm 0.33\%$ (Fig. 5). This does not represent physiologic variability but rather the variability due to the method of microsphere injection. Agreement (or method noise) is usually assessed by the correlation between simultaneous measures. Figure 5 also demonstrated that temporal heterogeneity occurs in as little as 30 s.

Regional perfusion remained relatively stable throughout the study period with high-flow regions receiving high flows throughout the experiment and low-flow regions consistently having lower flows. Figure 6 shows that over sample periods, regional perfusion showed little change. When examined by ANOVA for repeated measures there were no significant differences in the Pearson correlation coefficient (r) at any point during the study, $p > 0.05$ for all time points. On average, the r to the same lung piece separated by 5 min was 0.90 ± 0.07, at 20 min the r was 0.92 ± 0.04, at 20.5 min the r was $0.84 + 0.07$, at 20.5 min the r was 0.92 ± 0.03, at 40 min the r was $0.87 + 0.1$ and the r was $0.85 + 0.10$ at 60 min. Low flow regions had the greatest $CV_{temporal}$ (Fig. 7). The measure of temporal heterogeneity was corrected for the
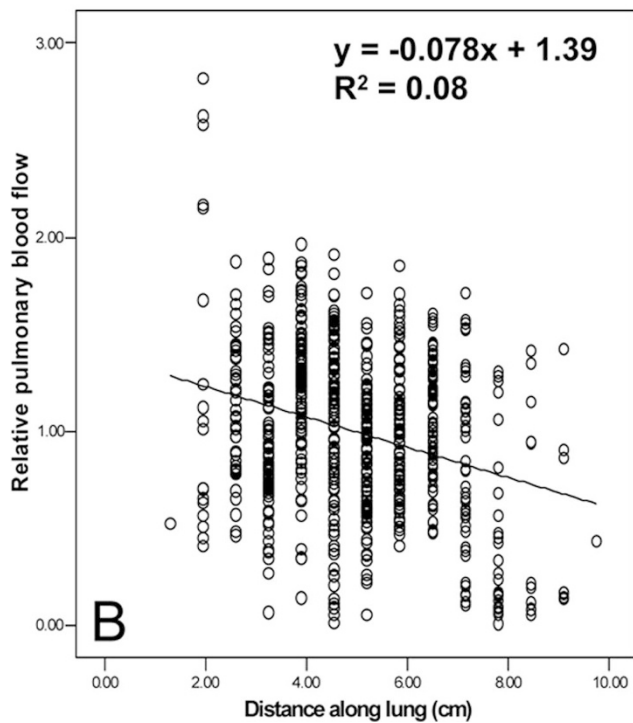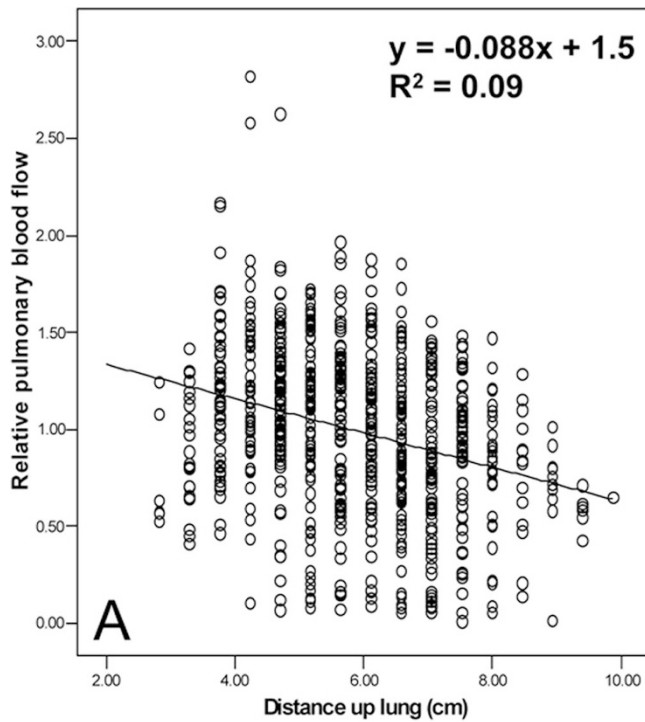
Figure 4. Directional gradient of PBF. *Panel A* shows a scattergraph of blood flow to individual pieces in a dorsal to ventral direction. *Panel B* shows PBF to individual pieces in a cephalad to caudad direction (piglet A). Regression lines show the decrease in regional PBF from dorsal to ventral and from cephalad to caudad.
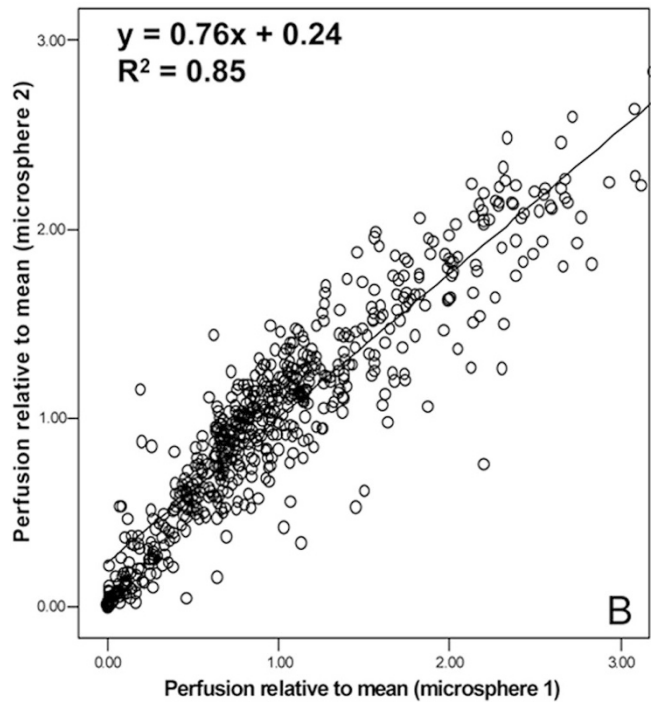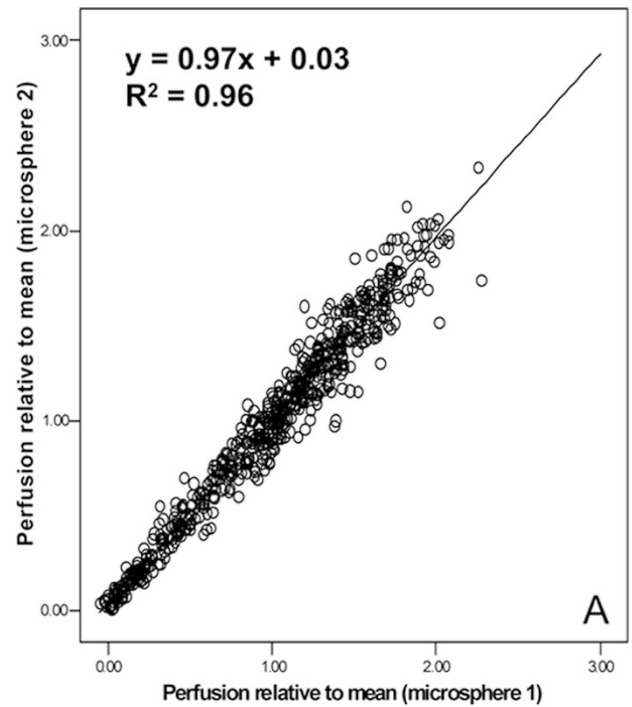

Figure 5. The error in method *vs* temporal variability. *Panel A* shows the simultaneous injection of two different colors of microspheres to demonstrate the error in the method. Linear correlation between the 2 measurements is good throughout the entire range of flows. *Panel B* shows the injection of two different colors of microspheres 30 s apart with much greater variability of flow throughout the entire range of flows. This decrease in correlation shows that temporal variability occurs even at 30 s (piglet C).

expected larger methodologic noise due to smaller numbers of microspheres depositing in low-flow regions by subtracting the CV_{method} from the $CV_{temporal}$ on a piece-by-piece basis.

DISCUSSION

Utilizing fluorescent microspheres to measure regional PBF, this study shows

1) Piglets have significant spatial variability in regional PBF even among isogravitational sections; 2) PBF follows a fractal pattern; 3) PBF decreases with distance from the hilum; and 4) PBF varies with time. This temporal variability or "twinkling" occurs over as little as 30 s. Both spatial and
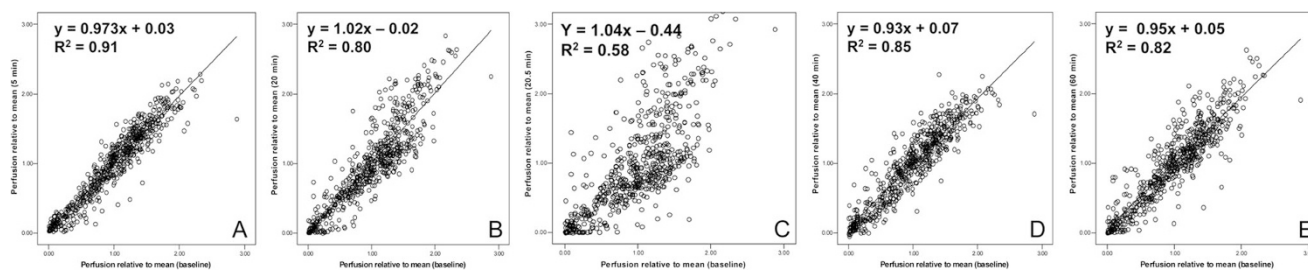
Figure 6. Comparison of regional pulmonary perfusion at different time intervals. Blood flow to each lung piece at a one-time point plotted against flow at baseline. Time between blood flow measurements is 5 (*A*), 20 (*B*), 20.5 (*C*), 40 (*D*) and 60 (*E*) minutes (piglet C). When data from all animals was evaluated, there was no significant change in correlation coefficients ($p < 0.05$ by ANOVA for repeated measures).
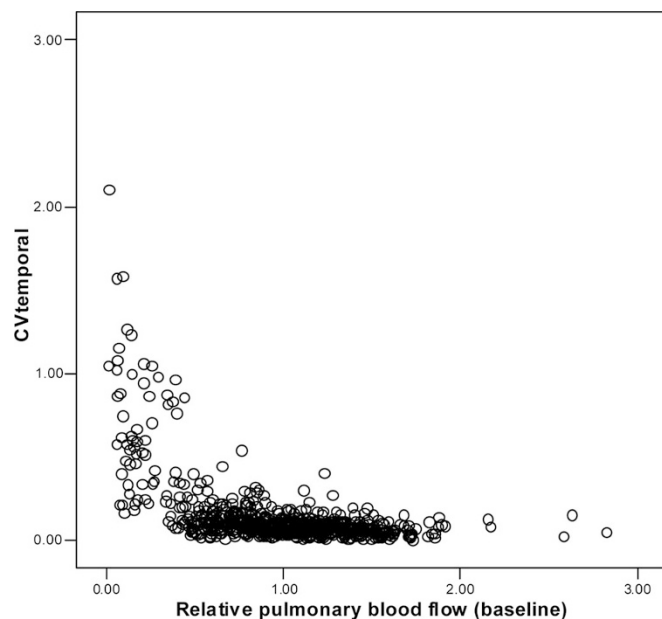

Figure 7. Relationship between temporal heterogeneity and flow per piece. $CV_{temporal}$ is shown as a function of average flow to piece. Most of the variability in flow over time occurs in low flow areas of the lung. Calculated $CV_{temporal}$ has been corrected for method noise (piglet A).

temporal variability appear to be greatest in the low-flow regions.

The fractal distribution of PBF appears more heterogeneous than proposed by the gravitational model (11). Like PBF, pulmonary ventilation is fractal in nature, with a similar extent of heterogeneity (17). This study establishes the fractal pattern of PBF among young animals. Despite the many differences described between the pulmonary vascular bed in young and adult animals (1–8) the underlying anatomic structure and organizing principle of PBF appears to be the same. Still the fractal dimension in these piglets is greater than in adult dogs which may be due, in part, to increased pulmonary vascular reactivity in neonatal animals (2,3,6,9). The difference in fractal dimension may also stem from changes in the anatomic pattern of vessel branching that develop postnatally. That is, with growth flow increases downstream of larger vessels and diminishes downstream from smaller vessels thus increasing spatial correlation and decreasing the fractal dimension. The $CV_{spatial}$ was greater in these piglets which would be expected since the smaller piece size should produce a greater heterogeneity than would be greater than in adults (18). The $CV_{spatial}$ was lower in these piglets than in dogs in contrast to our

hypothesis that due to the smaller piece size the heterogeneity would be greater than in adults probably due to species differences, although differences in maturation may be at play as well.

The hilar-peripheral gradient of PBF has also been found previously in a number of studies of adult animals including humans (9), dogs (19), sheep (20) and ponies (21) with contradictory evidence in dogs (22). A radial gradient is consistent with the fractal branching pattern of the pulmonary circulation in which vascular resistances is determined by the size of branching vessels and the length of circuit pathways. Regional PBF is determined primarily by the size of parent and grandparent vessels, which develops *in utero*.

Pulmonary blood flow in these piglets is also marked by temporal variability. Changes in the distribution of regional PBF occur over as little time as 30 s. Such variability suggests nearly continuous opening and closing of small pulmonary arterioles (twinkling). Although correlation in PBF decreases as the time in the study progressed, there are no obvious trends to the changes in pulmonary blood flow over time. The greatest temporal variation in regional pulmonary blood flow occurred in the regions with the lowest blood flow. Methodologic error is inversely proportional to the number of microspheres per piece (low flow regions). The variability in these pieces is due to methodologic noise. Since blood flow to those regions was low, small changes would be proportionately higher than to regions with higher blood flows. Due to the increased weight of methodological error, changes in pulmonary blood flow in low flow regions were corrected for methodological noise. In addition, the variability in pulmonary blood flow was stable over the time course of these studies. That is, the largest changes remained in the low flow areas throughout the study.

Just as with spatial heterogeneity, temporal heterogeneity of blood flow has also been widely demonstrated in adult animals. In addition to the finding in dog lungs (6), temporal heterogeneity of blood flow has been found in other organs including the brain, myocardium and skeletal muscle (23–25). The lower $CV_{temporal}$ results contradict our hypothesis that due to greater pulmonary vasoreactivity (2,3,6,8) temporal heterogeneity would be greater in piglets than in adult animals. The anatomic level of vascular reactivity measured in these studies may differ from the level responsible for temporal heterogeneity. Using videomicroscopic recordings Wagner *et al.* demonstrated temporal variation in PBF in a fractal pattern at the

level of the capillary that was independent of flow in neighboring alveolar regions (26). In larger vessels, high flow regions were near other high flow regions and low flow regions near other similar regions. So, the spatial correlation of blood flow may be determined by the geometry of larger vessels while other mechanisms may control the temporal fluctuations in blood flow.

Critique of methods. Fluorescent microspheres have been previously validated as a method for measuring regional pulmonary blood flow (27,28). We did not assess concentrations of microspheres in other organs as previous studies have shown that the microspheres are completely trapped by the pulmonary vasculature without altering local perfusion. The deposition of 15-μm accurately reflects regional PBF.

These anesthetized piglets were mechanically ventilated and studied in the supine position. Tidal volumes of 10–12 mL/kg were used in the study and while these volumes may have contributed to an increase in zone 1 conditions, gas exchange was stable throughout the experiment. Prior studies have shown that PBF heterogeneity did not change with induction of i.v. anesthesia and there were no significant changes in hemodynamic measurements during the course of the study (21). Spatial variability of PBF is higher in the supine than prone position and the majority of regional PBF heterogeneity is independent of posture, there is some redistribution is a gravitationally dependent manner (21,29). However, the estimation of temporal variability is probably lower than would be found in awake, active piglets when neurohumoral input to the pulmonary vasculature would be greater.

The observation of temporal perfusion heterogeneity depends on the duration of microsphere injection and the time interval of the injections. The microspheres in this study were injected over a 30-s period. If changes in pulmonary blood flow occur frequently, they may be averaged over the time period of the injection and consequently underestimated. Conversely, if changes occurred over periods of greater than 20 min, the $CV_{temporal}$ determined in this study would also be underestimated. We performed injections at time intervals of 30 s and 5 min. The $CV_{temporal}$ at these shorter time periods was similar to those measured at twenty minutes. Iverson and Nicolyasen (30) found that regional coronary vasodilation to occur over a wide range of cycle time, from 5 to 30 min. Glenny and colleagues (13) evaluated temporal changes in pulmonary blood flow in adult dogs at 20-min cycles. This study does not shed light on extremely rapid (<30 s) or slow (>20 min) changes.

The results of this study establish both spatial and temporal heterogeneity of regional pulmonary blood flow in the two-week old piglet. The fractal dimension in these piglets appears to be greater than that in adult animals but temporal and spatial heterogeneity are lower in piglets but of a similar magnitude. Although immature animals have a decreased pulmonary vascular reserve compared with adults, the innate anatomic structure and organizing principle of blood flow appears to be the same.

REFERENCES

1. Kelly DA, Hislop AA, Hall SM, Haworth SG 2002 Correlation of pulmonary arterial smooth muscle structure and reactivity during adaptation to extrauterine life. J Vasc Res 39:30–40
2. Redding GJ, McMurtry I, Reeves JT 1984 Effects of meclofenamate on pulmonary vascular resistance correlate with postnatal age in young piglets. Pediatr Res 18:579–583
3. Liu SF, Hislop AA, Haworth SG, Barnes PJ 1992 Developmental changes in endothelium-dependent pulmonary vasodilation in pigs. Br J Pharmacol 106:324–330
4. Owen-Thomas JB, Reeves JT 1969 Hypoxia and pulmonary arterial pressure in the rabbit. J Physiol 201:665–672
5. Gibson RL, Truog WE, Redding GJ 1988 Hypoxic pulmonary vasoconstriction during and after infusion of group B Streptococcus in neonatal piglets. Vascular pressure-flow analysis. Am Rev Respir Dis 137:774–778
6. Tyler T, Wallis R, Leffler C, Cassin S 1975 The effects of indomethacin on the pulmonary vascular response in the premature and mature newborn goat. Proc Soc Exp Biol Med 150:695–698
7. Rendas A, Branthwaite M, Lennox S, Reid L 1982 Response of the pulmonary circulation to acute hypoxia in the growing pig. J Appl Physiol 52:811–814
8. Reeves JT, Leathers JE 1964 Circulatory changes following birth of the calf and the effect of hypoxia. Circ Res 15:343–354
9. Hakim TS, Dean GW, Lisbona R 1987 Gravity independent inequality in pulmonary blood flow in humans. J Appl Physiol 63:1114–1121
10. Glenny RW, Robertson HT 1990 Fractal properties of pulmonary blood flow; characterization of spatial heterogeneity. J Appl Physiol 69:532–545
11. West JB, Dollery CT, Naimark A 1964 Distribution of blood flow in isolated lung; relation to vascular and alveolar pressures. J Appl Physiol 19:713–724
12. Glenny RW, Polissar NL, McKinney S, Robertson HT 1995 Temporal heterogeneity of regional pulmonary perfusion is spatially clustered. J Appl Physiol 79:986–1001
13. Glenny RW, Bernard S, Robertson HT 2000 Pulmonary blood flow remains fractal down to the level of gas exchange. J Appl Physiol 89:742–748
14. Haworth SG, Hislop AA 1981 Adaptation of the pulmonary circulation to extra-uterine life in the pig and its relevance to the human infant. Cardiovasc Res 15:108–119
15. Rendas A, Branthwaite M, Reid L 1978 Growth of pulmonary circulation in normal pig –structural analysis and cardiopulmonary function. J Appl Physiol 45:806–817
16. Glenny RW, Robertson HT 1991 Fractal modeling of pulmonary blood flow heterogeneity. J Appl Physiol 70:1024–1030
17. Altemeier WA, Robertson HT, Glenny RW 1998 Pulmonary gas exchange analysis by using simultaneous deposition of aerosolized and injected microspheres. J Appl Physiol 85:2344–2351
18. Hlastala MP, Chornuk MA, Self DA, Kallas HJ, Burns JW, Bernard S, Polissar NL, Glenny RW 1998 Pulmonary blood flow redistribution by increased gravitational force. J Appl Physiol 84:1278–1288
19. Glenny RW, Lamm WJ, Albert RK, Robertson HT 1991 Gravity is a minor determinant of pulmonary blood flow. J Appl Physiol 71:620–629
20. Walther SM, Domino KB, Glenny RW, Polissar NL, Hlastala MP 1997 Pulmonary blood flow distribution has a hilar-to-peripheral gradient in awake, prone sheep. J Appl Physiol 82:678–685
21. Jarvis KA, Steffey EP, Tyler WS, Willits N, Woliner M 1992 Pulmonary blood flow distribution in anesthetized ponies. J Appl Physiol 72:1173–1178
22. Nicolaysen G, Shephard J, Onizuka M, Tanita T, Hattner RS, Staub NC 1987 No gravity-independent gradient of blood flow distribution in dog lung. J Appl Physiol 63:540–545
23. Eke A, Herman P, Bassingthwaighte JB, Raymond GM, Balla I, Ikrenyi C 1997 Temporal fluctuations in regional red blood cell flux in the rat brain cortex is a fractal process. Adv Exp Med Biol 428:703–709 Plagiarism is bad
24. King RB, Bassingthwaighte JB 1989 Temporal fluctuations in regional myocardial flows. Pflugers Arch 413:336–342
25. Ellis CG, Wrigley SM, Groom AC 1994 Heterogeneity of red blood cell perfusion in capillary networks supplied by a single arteriole in resting skeletal muscle. Circ Res 75:357–368
26. Wagner WW Jr, Todoran TM, Tanabe N, Wagner TM, Tanner JA, Glenny RW, Presson RG Jr, 1999 Pulmonary capillary perfusion: intra-alveolar fractal patterns and interalveolar independence. J Appl Physiol 86:825–831
27. Glenny RW, Bernard S, Brinkley M 1993 Validation of fluorescent-labeled microspheres for measurement of region organ perfusion. J Appl Physiol 74:2585–2597
28. Lamm WJ, Bernard SL, Wagner WW Jr, Glenny RW 2005 Intravital microscopic observations of 15-microm microspheres lodging in the pulmonary microcirculation. J Appl Physiol 98:2242–2248
29. Altemeier WA, McKinney S, Krueger M, Glenny RW 2004 Effect of posture on regional gas exchange in pigs. J Appl Physiol 97:2104–2111
30. Iversen PO, Nicolaysen G 1989 Heterogeneous blood flow distribution within single skeletal muscles in the rabbit: role of vasomotion, sympathetic nerve activity and effect of vasodilation. Acta Physiol Scand 137:125–133